Substitution of (13) into (62) yields

$$\Delta f_{k+1} = (1 - \psi)\Delta f_k + O_7(\varepsilon) + O_6(\epsilon)\Delta\overline{u}_k. \quad (63)$$

Increasing k leads to $\varepsilon \to 0$. In addition, $\Delta\overline{u}_k$ is bounded in the sense of L^2-norm. Therefore, it is proved from (63) that f_k converge to f_d in the sense of L^2-norm as $k \to \infty$ if the learning gain ψ is selected so that it satisfies $0 < \psi < 1$. This proves Theorem 3.

REFERENCES

[1] S. Arimoto, S. Kawamura, and F. Miyazaki, "Bettering operation of robots by learning," *J. Robotic Syst.*, vol. 1, no. 2, pp. 123–140, 1984.

[2] S. Kawamura, F. Miyazaki, and S. Arimoto, "Realization of robot motion based on a learning method," *IEEE Trans. Syst., Man and Cybern.*, vol. 18, no. 1, pp. 126–134, 1988.

[3] G. Heinzinger, D. Fenwick, B. Paden, and F. Miyazaki, "Stability of learning control with disturbances and uncertain initial conditions," *IEEE Trans. Automat. Cont.*, vol. 37, no. 1, pp. 110–114, 1992.

[4] P. Bondi, G. Casalino, and L. Gambardella, "On the iterative learning control theory for robotic manipulators," *IEEE J. Robot. and Automat.*, vol. 4, no. 1, pp. 14–22, 1988.

[5] S. Kawamura, F. Miyazaki, and S. Arimoto, "Hybrid position/force control of robot manipulators based on learning method," in *Proc. '85 Int. Conf. on Advanced Robotics*, 1985, pp. 235–242.

[6] D. Jeon and M. Tomizuka, "Learning hybrid force and position control of robot manipulators," *IEEE Trans. on Robot. and Automat.*, vol. 9, no. 4, pp. 423–431, 1993.

[7] M. Aicardi, G. Cannata, and G. Casalino, "A learning procedure for position and force control of constrained manipulators," in *Fifth Int. Conf. Advanced Robot. (ICAR)*, 1991, pp. 423-430.

[8] P. Lucibello, "A learning algorithm for hybrid force control of robot arms," in *Proc. IEEE Int. Conf. Robot. and Automati.*, 1993, pp. 654–658.

[9] S. Arimoto and T. Naniwa, "Learning control for robot tasks under geometric endpoint constraints," in *Proc. IEEE Int. Conf. on Robot. and Automat.*, 1992, pp. 1914–1919.

[10] S. Arimoto, T. Naniwa, and T. Tsubouchi, "Principle of orthogonalization for hybrid control of robot manipulators," in *Proc. IMACS'92 (Int. Symp. Robot., Mechatronics, and Manufact. Syst. '92 Kobe)*, 1992, pp. 1293–1300.

[11] J. Baumgarte, "Stabilization of constraint and integrals of motion in dynamical systems," *Comput. Methods in Appl. Mech. and Eng.*, vol. 1, pp. 1–16, 1972.

[12] D.-S. Bae and S.-M. Yang, "A stabilization method for kinematic and kinetic constraint equations," in *NATO ASI Series Vol. F69: Real-Time Integration Methods for Mechanical Systems Simulation*, E. J. Haug and R. C. Deyo, Eds. New York: Springer-Verlag, 1990, pp. 209–232.

[13] W. H. Raivert and J. J. Craig, "Hybrid position/force control of manipulators," *ASME J. Dynamic Syst., Measurement, and Cont.*, vol. 103, no. 2, pp. 126–133, 1981.

[14] N. H. McClamroch and D. Wang, "Feedback stabilization and tracking of constrained manipulators," *IEEE Trans. Automat. Cont.*, vol. 33, no. 5, pp. 419–426, 1988.

[15] O. Khatib, "A unified approach for motion and force control of robot manipulators: The operational space formulation," *IEEE J. Robot. and Automat.*, vol. 3, no. 1, pp. 43–53, 1987.

[16] C. G. Atkeson and J. McIntyre, "Robot trajectory learning through practice," in *Proc. IEEE Int. Conf. Robot. and Automat.*, 1986, pp. 1737–1742.

[17] S. Arimoto, T. Naniwa, and H. Suzuki, "Selective learning with a forgetting factor for robotic motion control," in *Proc. IEEE Int. Conf. Robot. and Automat.*, 1991, pp. 728–733.

[18] S. Arimoto, Y. H. Liu, and T. Naniwa, "Principle of orthogonalization for hybrid control of robot arms," in *Proc. 12th IFAC World Cong.*, 1993, vol. 1, pp. 507–512.

Primitives for Smoothing Mobile Robot Trajectories

Sara Fleury, Philippe Souères, Jean-Paul Laumond, and Raja Chatila

***Abstract*— Clothoids are very useful for smoothing the motion of a mobile robot moving along a trajectory. This paper addresses the problem of smoothing mobile robot motions when cusps, i.e., changes of motion direction along the trajectory, are imposed. We pinpoint some special curves (that we call "anticlothoids") and we discuss how they can be used together with clothoids in order to smooth a predefined trajectory.**

I. INTRODUCTION

Clothoids (or Cornu spirals) are known as very useful curves for smoothing trajectories. Their equation is $\kappa = k_c s + \kappa_0$ where κ is the curvature, s the arc length, κ_0 the initial curvature and k_c a constant characterizing the shape of the clothoid. Clothoids allow to link curves of infinite radius of curvature (i.e., lines) and curves of finite radius of curvature, with a continuous change of the curvature. Clothoids have practical applications in railway and highway design. They have been introduced in Robotics ([1]–[3]) for smoothing the trajectories of a mobile robot moving "forward" on a broken line (i.e., without a change of orientation along the trajectory).

This paper introduces the *involutes of circles*.[1] The natural equation of an involute of a circle is $\rho^2 = 2k_a s$, ρ being the radius of curvature and k_a the radius of the circle. Another general form of this equation is $\rho = k_a(\theta - \theta_0) + \rho_0$ where θ is the direction of the tangent to the curve, θ_0 it's initial direction[2] and ρ_0 the initial radius of curvature. k_a is the characteristic parameter of the involute. Such curves allow to link "curves" of infinite curvature (i.e., curves reduced to a point) and curves of finite curvature, with a continuous change of the curvature. This property of the circle involutes leads us to call them *anticlothoids* in the context of this paper.

Like clothoids, anticlothoids are the time-optimal trajectories of a two driving wheels mobile robot [5]. Both types of curves are dual from the point of view of control. They are produced by applying, respectively, a same constant acceleration on both wheels (anticlothoids) or constant and opposite accelerations (clothoids). The purpose of this paper is to show how to use anticlothoids in order to smooth the motions of a mobile robot when *cusps* are imposed (i.e., when the robot has to change the direction of its motion).

We shall first overview some known results on trajectory smoothing, mainly using clothoids (Section II). Then we introduce both types of curves from a control theory viewpoint, and we show how a mobile robot can execute trajectories including them (Section III).

Geometric properties are then proven (Section IV). Two connected oriented straight line segments being given as a reference trajectory, we show how to plan a motion such that:

1) The velocities of the driving wheels are continuous and never simultaneously null (i.e., the motion is smooth).

Manuscript received August 6, 1993; revised July 10, 1994. A first version of this paper was presented at the IEEE International Conference on Robotics and Automation 1993, Atlanta, GA. This work was supported by the ECC Esprit 3 Project 6546 PROMotion.

The authors are with LAAS-CNRS, 7 Avenue du Colonel Roche, 31077 Toulouse, France.

IEEE Log Number 9410113.

[1] The involute of a circle is the curve described by the end of a thread as it is unwound from a stationary spool [4].

[2] As s is a measure of the length of the curve, $(\theta - \theta_0)$ measures the angular variation of the curve.

2) The trajectory never lies farther than a fixed threshold from the segments (this condition is required for collision avoidance).
3) The produced trajectory respects the imposed directions of motion.

The trajectories will consist of sequences of clothoids and anti-clothoids.

In Section V, we sketch a method for smoothing a mobile robot's trajectory consisting of a polygonal line, while accounting for non-collision and direction changes.

II. Related Work

Clothoids are extensively used for the design of highways [6] in order to smoothly join straight lines with circular portions. They are also used as splines in Computer Aided Design (CAD) [7].

They were more recently introduced in Robotics. Indeed, most trajectory planners produce trajectories consisting of straight lines and turns that force the robot to stop, because of the discontinuity in the angular speed when the direction changes. In order to eliminate these stops, smoothing the reference trajectory to produce a swift motion has been a long-time objective, for which the use of clothoids is very popular.

The smoothing problem was also addressed for producing directly a trajectory that joins a sequence of robot configurations $\{(x, y, \theta)_i\}$ without stopping.

This problem has been addressed by Iijima *et al.* [1] where clothoid curves were exhibited as transition trajectories. The use of clothoids was also studied and implemented on the mobile robot Hilare [2], [8] for smoothing a path consisting of straight lines and turns.

In [3], Kanayama and Miyake join initial and final configurations by a broken line that is used as an entry to a smoothing algorithm which produces sequences of clothoid arcs and straight lines.

Shin and Singh [9] address a similar problem with the additional constraint of a lower bounded turning radius. They produce a smooth path composed of clothoid arcs only.

In [10], Kanayama and Hartman propose the use of cubic spirals for obtaining smooth trajectories linking a sequence of configurations two by two. They propose a criterion for smoothness (a quadratic function of the curvature or of its derivative). The use of cubic spirals produces trajectories of a larger curvature radius than in the case of clothoids, thus producing a "smoother" motion.

Delingette *et al.* [11] generalize the smoothing problem in order to take into account specified end conditions as well as a limited turning radius by adding control points to the trajectory. This is much similar to the approaches in CAD. They introduced "intrinsic splines," curves whose curvature is a polynomial function of the arc length. These curves are generalizations of the clothoids and cubic spirals. See also the work of Segovia et al. on the use of Bezier's curves for this concern [12].

To our knowledge, the involutes of circles were never exploited for smoothing purposes. They actually correspond to the smoothing of *cusps* (seldom encountered in highways ...). In robotics however, the generation of collision-free trajectories sometimes imposes such constraints. As we shall see, the involute of a circle then becomes a very useful curve.

III. Clothoids and Anticlothoids

A. Time-Optimal Trajectories for a Two Driving Wheel Mobile Robot

Let us consider mobile robots whose locomotion system consists of two parallel independent driving wheels (e.g., the three mobile robots of the Hilare family developed at LAAS [13]). The length of the axis supporting the wheels is noted d. The reference point of the robot is the midpoint of the axis. Its coordinates are denoted by (x, y). The direction of the vehicle is noted θ. Therefore, a configuration of the robot is a triple $(x, y, \theta) \in (\mathbf{R}^2 \times S^1)$. We denote by v_r and v_l the linear velocities of the right and left wheels, respectively, (see Fig. 1). The robot can then be modeled by the following control system:

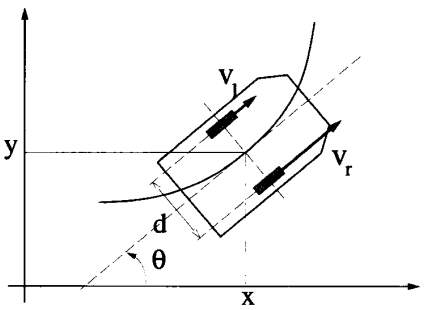

Fig. 1. Kinematics of Hilare 2.

$$\begin{pmatrix} \dot{x} \\ \dot{y} \\ \dot{\theta} \\ \dot{v}_r \\ \dot{v}_l \end{pmatrix} = \begin{pmatrix} \frac{1}{2}(v_r + v_l)\cos\theta \\ \frac{1}{2}(v_r + v_l)\sin\theta \\ \frac{1}{d}(v_r - v_l) \\ 0 \\ 0 \end{pmatrix} + \begin{pmatrix} 0 \\ 0 \\ 0 \\ 1 \\ 0 \end{pmatrix} u_r + \begin{pmatrix} 0 \\ 0 \\ 0 \\ 0 \\ 1 \end{pmatrix} u_l$$

Moreover, the accelerations u_r and u_l of the wheels (i.e. the inputs of the system) are assumed to be bounded: $|u_r| \leq a$ and $|u_l| \leq a$.

By applying the Maximum Principle (from optimal control theory [14]), one can prove that the time-optimal controls of the above system verify $|u_r| = |u_l| = a$ [5], [15]. Thus the time-optimal trajectories are supported by two types of curves corresponding, respectively, to the cases $u_r = u_l$ and $u_r = -u_l$.

Remarks:

1) This result does not characterize the shape of the time-optimal trajectories linking two given configurations. It just gives necessary conditions for a trajectory to be time optimal (i.e., it shows how the optimal trajectory looks like *locally*). At this moment, providing sufficient conditions of optimality is still an open problem (see [15] for a numerical approach to the problem). Notice that necessary and sufficient conditions have been found recently for the car-like robot [15].
2) We can relate u_r and u_l to the linear and angular accelerations $\dot{v}$ and $\dot{\omega}$ by the following equation:

$$\begin{pmatrix} \dot{v} \\ \dot{\omega} \end{pmatrix} = \begin{pmatrix} 1/2 & 1/2 \\ 1/d & -1/d \end{pmatrix} \begin{pmatrix} u_r \\ u_l \end{pmatrix}$$

Thus, the optimal trajectories presented here are not only valid for the two-driving wheels mobile robots, but also for any system with linear and angular acceleration controls, without constraints on the curvature.

Now we show that the two types of curves have dual geometric properties, as announced in the introduction.

Notations: A motion of the robot consists of two mappings $u_r$and u_l from a time interval $[0, 1]$ onto $\{-a, a\}$. The corresponding trajectory of the robot (i.e., the locus of the point (x, y) in the plane) is noted γ. γ is a mapping from $[0, 1]$ onto the plane $\mathbf{R}^2$. The arc length from $\gamma(0)$ to $\gamma(t)$ is noted $s(t)$. The curvature at a point $\gamma(t)$ is noted $\kappa(t)$, while the radius of curvature is $\rho(t) = 1/\kappa(t)$. The linear and angular velocities are, respectively, noted $v(t)$ and $\omega(t)$. The direction of the tangent to γ at some point $\gamma(t)$ (when it is defined) is the direction θ of the vehicle at this point, i.e., $\omega(t) = \dot{\theta}(t)$. Finally recall that $\rho(t) = v(t)/\omega(t)$.

All the initial values $v(0)$, $\omega(0)$, $\theta(0)$... are noted v_0, ω_0, θ_0... The final values are noted v_1, ω_1, θ_1...

B. Case $u_r = -u_l$: The Clothoids

Let us consider two constant controls verifying $u_r(t) = -u_l(t)$. In this case $\dot{v}(t) = \frac{1}{2}(\dot{v}_r(t) + \dot{v}_l(t)) = 0$. $v(t)$ is constant and equal to v_0. Then $s(t) = v_0 t$.

Now, $\dot{v}_r(t) = \pm a$ while $\dot{v}_l(t) = \mp a$. By integration, $v_r(t) = \pm at + v_{r0}$, $v_l(t) = \mp at + v_{l0}$ and $\omega(t) = \dot{\theta}(t) = \pm\frac{2a}{d}t + \omega_0$.

Therefore,

$$\kappa(t) = \frac{\pm\frac{2a}{d}t + \omega_0}{v_0} = \pm\frac{2a}{dv_0^2}s(t) + \frac{\omega_0}{v_0}. \quad (1)$$

The curve is a clothoid whose characteristic constant k_c is $\frac{2a}{dv_0^2}$.

When $\omega_0 = \theta_0 = 0$, the coordinates of a point $\gamma(t)$ are given by the Fresnel integrals (see [4] for instance):

$$x(t) = \mathrm{sgn}(v_0)\sqrt{\frac{\pi}{k_c}}\int_0^{\sqrt{\frac{2a}{d\pi}}t} \cos\frac{\pi}{2}u^2\,du$$

$$= \mathrm{sgn}(v_0)\sqrt{\frac{\pi}{k_c}}CF(\sqrt{\frac{2a}{d\pi}}t) \quad (2)$$

$$y(t) = \mathrm{sgn}(v_0u_r)\sqrt{\frac{\pi}{k_c}}\int_0^{\sqrt{\frac{2a}{d\pi}}t} \sin\frac{\pi}{2}u^2\,du$$

$$= \mathrm{sgn}(v_0u_r)\sqrt{\frac{\pi}{k_c}}SF(\sqrt{\frac{2a}{d\pi}}t) \quad (3)$$

The tangent direction at this point is

$$\theta(t) = \mathrm{sgn}(u_r)\frac{a}{d}t^2. \quad (4)$$

Fig. 2 shows a clothoid curve for $u_r > 0$. For an initial configuration $(0,0,0)$ the upper part is described for $v_0 > 0$, and the lower part for $v_0 < 0$. A curve symmetrical with respect to the Ox axis is obtained for $u_r < 0$. Computation of the coordinates when $\omega_0 \neq 0$ is easily done from the above system.

Remarks:

1) In the computations above, we assume $v_0 \neq 0$. When $v_0 = 0$, direct computations show that γ corresponds to a rotation[3]. Rotations can then be viewed as degenerated clothoids with infinite characteristic constants (i.e., points).
2) The linear velocity v is constant along a clothoid.
3) Equation (1) shows that clothoids can link smoothly curves of zero curvature (lines) and curves with non zero curvature.

C. Case $u_r = u_l$: The Anticlothoids

Now, let us consider two constant controls verifying $u_r(t) = u_l(t)$. In this case, we have $\dot{\omega}(t) = \frac{1}{d}(\dot{v}_r(t) - \dot{v}_l(t)) = 0$ and $\omega(t)$ is constant and equal to ω_0. Thus, $\theta(t) = \omega_0 t + \theta_0$.

The acceleration $\dot{v}(t)$ equals $\mathrm{sgn}(u_r)a$. Thus, $v(t) = \mathrm{sgn}(u_r)at + v_0$. Therefore,

$$\rho(t) = \frac{v(t)}{\omega(t)} = \frac{\mathrm{sgn}(u_r)at + v_0}{\omega_0} = \mathrm{sgn}(u_r)\frac{a}{\omega_0^2}(\theta(t) - \theta_0) + \frac{v_0}{\omega_0}. \quad (5)$$

The curve is an anticlothoid whose characteristic constant is $k_a = a/\omega_0^2$.

When $v_0 = \theta_0 = 0$, the coordinates of a point $\gamma(t)$ are given by the following parametric system:

$$x(t) = \mathrm{sgn}(u_r)k_a(\cos(\omega_0 t) + \omega_0 t\sin(\omega_0 t) - 1) \quad (6)$$

$$y(t) = \mathrm{sgn}(u_r)k_a(\sin(\omega_0 t) - \omega_0 t\cos(\omega_0 t)) \quad (7)$$

The tangent direction at this point is

$$\theta(t) = \omega_0 t. \quad (8)$$

[3]In this paper, a *rotation* always designates a turn about the robot's own center (axis).

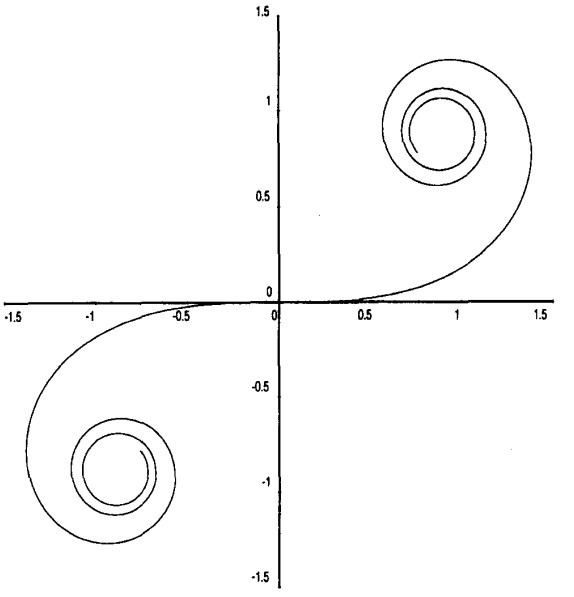

Fig. 2. A clothoid for $u_r = +a$.

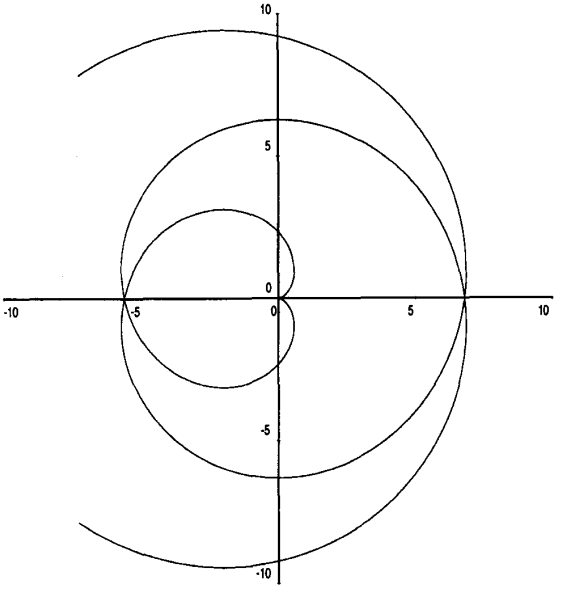

Fig. 3. An anticlothoid $u_r = +a$.

Fig. 3 shows an anticlothoid curve for $u_r > 0$. For an initial configuration $(0,0,0)$, a positive ω_0 causes a counterclockwise motion, whereas a negative ω_0 causes a clockwise motion. A curve symmetric with respect to the origin is obtained for $u_r < 0$. The computation of the coordinates for the general case ($v_0 \neq 0$, $\theta_0 \neq 0$) is given in the appendix.

Remarks:

1) When $\omega_0 = 0$, γ is a line. Lines appear as degenerated anticlothoids with infinite characteristic constants.
2) The angular velocity ω is constant along an anticlothoid.
3) Equation (5) shows that anticlothoids can link smoothly curves with zero radius of curvature to curves with a non zero curvature radius.

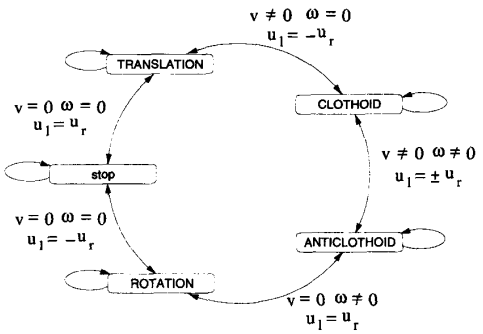

Fig. 4. Possible combinations of clothoids and anticlothoids.

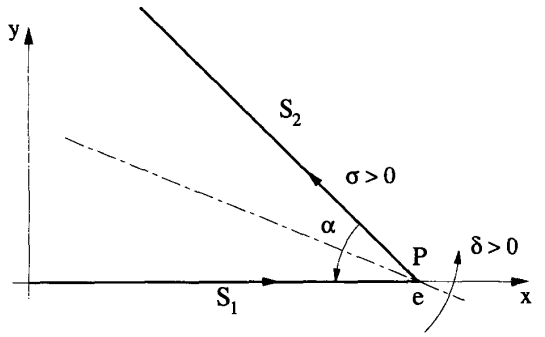

Fig. 5. Inputs of the problem.

4) While anticlothoids and clothoids are dual curves from the control theory point of view, the first ones are analytic curves and the second ones are not.

D. How to Link Clothoids and Anticlothoids?

Any motion starts with $v_0 = \omega_0 = 0$ and ends with $v_1 = \omega_1 = 0$. This means that any motion provided by optimal controls starts and ends either with a rotation or a translation.

Moreover, since the angular velocity is zero along a line, the piece of trajectory after or before a line, if any, is necessarily a clothoid. In the same way, the portion after or before a rotation is necessarily an anticlothoid.

Fig. 4 shows all the possible combinations linking clothoids and anticlothoids. The type of trajectories are the nodes of the graph, while the conditions of switching are the arcs.

Now, let us consider a trajectory γ consisting of an arc of clothoid followed by an arc of anticlothoid, such that $\omega_0 = 0$ and $v_1 = 0$. Such a trajectory links a translation and a rotation (we fix $\theta_0 = 0$). Let $\tau \in [0, 1]$ such that $\gamma(\tau)$ is the meeting point of the two arcs. We note $\theta(\tau), \omega(\tau), v(\tau)$, respectively, θ_τ, ω_τ, and v_τ.

With $u_r > 0$, we have from (4), $\theta_\tau = \frac{a}{d}\tau^2$. From (8), $\theta_1 = (1-\tau)\omega_\tau + \theta_\tau$. Because the linear velocity is constant along a clothoid, $v_\tau = v_0$. Now, $v_1 = 0$, thus $v_0 = (1-\tau)a$. Because the angular velocity is constant along an anticlothoid and $\omega_0 = 0$, we have $\omega_1 = \omega_\tau = \frac{2a}{d}\tau$.

The characteristic constants of the clothoid and the anticlothoid are, respectively, $k_c = \frac{2a}{dv_0^2}$ and $k_a = \frac{a}{\omega_1^2}$. Thus:

$$\theta_\tau = \frac{d\omega_1^2}{4a} = \frac{d}{4k_a} \tag{9}$$

$$\theta_1 = \theta_\tau + \frac{\omega_1 v_0}{a} = \frac{d}{4k_a} + \sqrt{\frac{2}{dk_c k_a}} \tag{10}$$

Equation (10) gives the angular variation along γ as a function of the characteristic parameters k_a and k_c. It is used for proving the correctness of the smoothing primitives below.

IV. Four Primitives for Smoothing Paths and their Geometric Properties

Consider a collision-free trajectory consisting of a sequence of straight-line directed segments. The direction of the segments gives the direction of the movement (forward or backward). The endpoints of the segments are also directed according to the direction of the rotations at these points. Such a trajectory can be *a priori* given to the robot by a user or provided by some motion planner (e.g. [17] and [18] for a more complete review).

Linking a translation and a rotation forces the robot to stop. At the stop point, *both* linear and angular velocities v and ω are zero. The trajectory appears as a sequence such as (Stop–TRANSLATION–Stop–ROTATION–Stop–TRANSLATION–...–Stop)[4]. The goal of the smoothing is to remove the stop points, while maintaining the continuity of the velocities v and ω, and controlling the deviation of the trajectory after smoothing from the initial one. At any point of the resulting trajectory, either ω or v are non zero.

A. The Canonical Motion [T-s-R-s-T]

For this purpose, we introduce canonical primitives for smoothing subsequences of trajectory such as [TRANSLATION–Stop–ROTATION–Stop–TRANSLATION] (or [T-s-R-s-T]). We want to produce a smooth trajectory symmetric with respect to the bisector of the lines supporting consecutive translations separated by a rotation.

Notations: We note S_1 the first straight line segment and S_2 the second one (see Fig. 5). P is the point of intersection of S_1 and S_2. α is the measure of the angle of the two lines supporting S_1 and S_2 ($0 < \alpha < \pi$; the case $\alpha < 0$ can be deduced by symmetry). Moreover we assume that the direction of motion on S_1 is positive (i.e., the robot moves forward). The case of a backward motion can also be deduced by symmetry. We note σ the direction of motion on S_2: $\sigma = 1$ if the robot moves forward and $\sigma = -1$ otherwise. Finally, δ is the direction of rotation at P: $\delta = 1$ if the robot rotates counterclockwise and $\delta = -1$ otherwise.

The inputs of the problem are an elementary sequence [T–s–R–s–T] and a safety parameter defined for collision avoidance, i.e.:

- Two straight line segments S_1 and S_2, intersecting at P with angle α and e= min [length (S_1, S_2)].
- σ the imposed direction of motion on S_2.
- δ the imposed direction of rotation at P.
- A positive number ϵ measuring the maximum deviation between the reference trajectory (S_1, S_2), and the resulting smoothed trajectory.

The output is a trajectory γ such that:

- The initial and final configurations of γ are the initial and final configurations of the input trajectory.
- γ is symmetric with respect to the bisector (S_1, S_2).
- The velocities of the wheels of the mobile robot moving along γ are continuous and never simultaneously null.
- The variation of the vehicle direction along γ is *exactly* the variation of the vehicle direction during the rotation, with the sign of δ.
- The distance from any point on γ to the reference trajectory (S_1, S_2) is never greater than ϵ.

According to the directions of motion on S_2 ($\sigma = \pm 1$) and during the rotation ($\delta = \pm 1$), we have to consider four cases.

[4] or: (Stop–ROTATION–Stop–TRANSLATION–...–Stop)

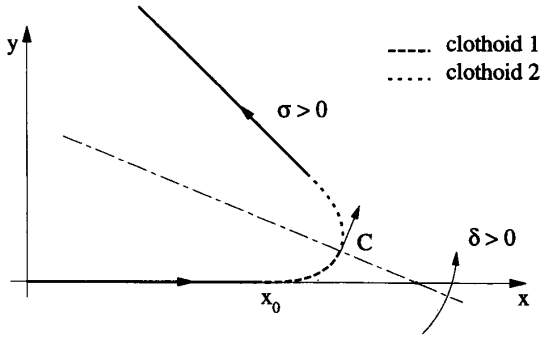

Fig. 6. The turn.

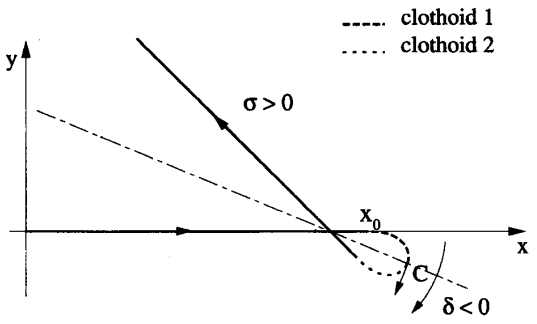

Fig. 7. The loop.

In all cases, the trajectories to compute must start and end at configurations with zero curvature. Therefore, the initial and final portions of the trajectories are arcs of clothoids.

When $\sigma = -1$, the linear velocity of the robot has to be zero at some point because of its direction change. Thus, the trajectories to compute will contain arcs of anticlothoids.

B. $\sigma = 1$ and $\delta = 1$: The Turn

This is a classical case. The smoothing primitive consists of two arcs of clothoid that meet at a configuration c such that

$$\begin{cases} x_c = e - \epsilon \cot \frac{\alpha}{2} \\ y_c = \epsilon \\ \theta_c = \frac{\pi - \alpha}{2} \end{cases}.$$

We want to compute an arc of clothoid linking the x-axis to c. From (4) we can substitute t by $\sqrt{\frac{d\theta_c}{a}}$ in (2) and (3):

$$x_c = \sqrt{\frac{\pi}{k_c}} CF\left(\sqrt{\frac{2\theta_c}{\pi}}\right) + x_0$$
$$y_c = \sqrt{\frac{\pi}{k_c}} SF\left(\sqrt{\frac{2\theta_c}{\pi}}\right)$$

$(x_0, 0, 0)$ is the initial configuration of the clothoid. Now, we have to compute k_c and x_0:

$$x_0 = e - \epsilon \left(\cot \frac{\alpha}{2} + CF\left(\sqrt{\frac{\pi - \alpha}{\pi}}\right) / SF\left(\sqrt{\frac{\pi - \alpha}{\pi}}\right) \right)$$
$$k_c = \frac{\pi}{c^2} SF\left(\sqrt{\frac{\pi - \alpha}{\pi}}\right)$$

The first clothoid arc is then computed. The second one is deduced by symmetry. Fig. 6 shows the resulting smoothed trajectory.

C. $\sigma = 1$ and $\delta = -1$: The Loop

This (less classical) case is similarly processed by reasoning from the intermediate configuration c. the result is a *loop* composed of two clothoid arcs (see Fig. 7):

$$\begin{cases} x_c = e + \epsilon \cos \frac{\alpha}{2} \\ y_c = -\epsilon \sin \frac{\alpha}{2} \\ \theta_c = -\frac{\pi + \alpha}{2} \end{cases}$$

D. $\sigma = -1$ and $\delta = 1$: The Internal Cusp

The case of cusps is more complicated. The smoothing primitive consists of two arcs of clothoid linked by two arcs of anticlothoid, symmetric with respect to the bisector of S_1 and S_2.

Consider the configuration c lying on the bisector and verifying:

$$\begin{cases} x_c = e - \epsilon \cot \frac{\alpha}{2} \\ y_c = \epsilon \\ \theta_c = \frac{2\pi - \alpha}{2} \end{cases}$$

We build a sequence consisting of an arc of a clothoid and an arc of an anticlothoid starting from the x-axis to c.

Let $\tilde{c}$ be the configuration at the switch between the clothoid and the anticlothoid. Being the meeting point of a clothoid and an anticlothoid, $\tilde{c}$ verifies (9) and

$$\begin{aligned} x_{\tilde{c}} &= \sqrt{\frac{\pi}{k_c}} CF\left(\sqrt{\frac{2\theta_{\tilde{c}}}{\pi}}\right) + x_0 \\ y_{\tilde{c}} &= \sqrt{\frac{\pi}{k_c}} SF\left(\sqrt{\frac{2\theta_{\tilde{c}}}{\pi}}\right) \\ \text{with } \theta_{\tilde{c}} &= \frac{d}{4k_a} \end{aligned}$$

Now, c is the endpoint of an arc of an anticlothoid whose initial configuration is $\tilde{c}$. From the computations done in Section III-D (see (10)) and in the appendix ((11) and (12)):

$$\begin{cases} x_c = k_a(\cos\theta_c - \cos\theta_{\tilde{c}} + (\theta_c - \theta_{\tilde{c}})\sin\theta_{\tilde{c}}) + x_{\tilde{c}} \\ y_c = k_a(\sin\theta_c - \sin\theta_{\tilde{c}} - (\theta_c - \theta_{\tilde{c}})\cos\theta_{\tilde{c}}) + y_{\tilde{c}} \\ \theta_c = \frac{d}{4k_a} + \sqrt{\frac{2}{dk_c k_a}} \end{cases}$$

Therefore the indeterminates x_0, k_a and k_c verify the following system:

$$\begin{cases} e - \epsilon \cot \frac{\alpha}{2} = k_a\left(\cos\theta_c - \cos\frac{d}{4k_a} + \sqrt{\frac{2}{dk_c k_a}} \sin\frac{d}{4k_a}\right) \\ \qquad + \sqrt{\frac{\pi}{k_c}} CF\left(\sqrt{\frac{d}{2k_a\pi}}\right) + x_0 \\ \epsilon = k_a\left(\sin\theta_c - \sin\frac{d}{4k_a} - \sqrt{\frac{2}{dk_c k_a}} \cos\frac{d}{4k_a}\right) \\ \qquad + \sqrt{\frac{\pi}{k_c}} SF\left(\sqrt{\frac{d}{2k_a\pi}}\right) \\ \frac{2\pi - \alpha}{2} = \frac{d}{4k_a} + \sqrt{\frac{2}{dk_c k_a}} \end{cases}$$

From the third equation we can compute k_c as a function of k_a. By replacing k_c in the second equation, we obtain an equation with the only indeterminate k_a. We solve this new equation numerically. Finally x_0 is given by the first equation.

Fig. 8 shows an example of trajectory composed of this primitive.

E. $\sigma = -1$ and $\delta = -1$: The External Cusp

Here, the primitive is exactly the same as the previous one, except that we consider the intermediate following configuration c (Fig. 9):

$$\begin{cases} x_c = e + \epsilon \cos \frac{\alpha}{2} \\ y_c = -\epsilon \sin \frac{\alpha}{2} \\ \theta_c = -\frac{\alpha}{2} \end{cases}$$

The smoothed trajectory lies on the other side of the reference trajectory (S_1, S_2) (Fig. 9).

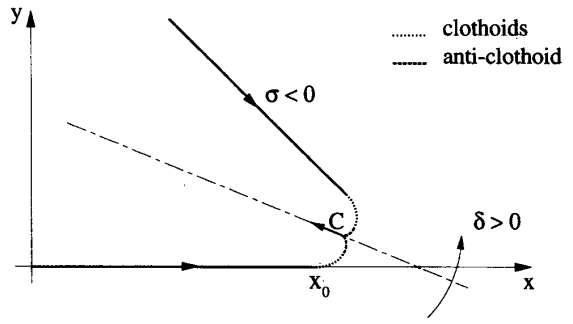

Fig. 8. The internal cusp.

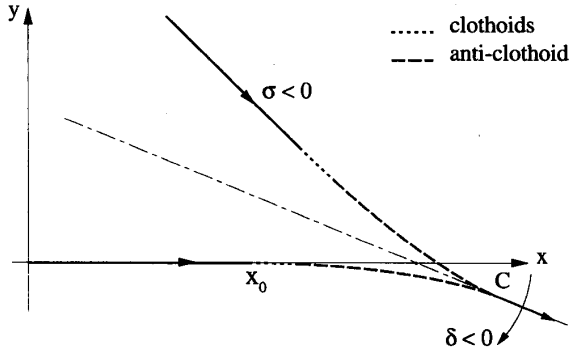

Fig. 9. The external cusp.

F. Comments

In situations geometrically very constrained, the length e of S_1 may be too small and the above computations may lead to $x_0 < 0$. In this case, we fix x_0 to zero. ϵ becomes an indeterminate which can be computed. The final trajectory will then be closer to the segments than the initial geometric constraints of the input ϵ.

We have studied the case of $\alpha \in]0..\pi[$. The case $\alpha \in]\pi..2\pi[$ can be deduced by symmetry by changing the sign of δ. The transition between the two intervals (for $\alpha = 0$ and $\alpha = \pi$) induces a switch between a *loop* and a *turn* or between an *internal* and an *external* cusp. The change in the nature of the smoothing primitives could be interpreted as an "instability" of the resulting trajectory. In the case of the cusp with $\alpha = 0$ however, the transformation between the internal and the external cusp is continuous.

G. Geometrical Property for Collision Avoidance

All the above trajectories are clearly produced by smooth controls. According to the kinematic properties of the motions along clothoids and anticlothoids, the velocities of the wheels of the mobile robot are never zero simultaneously.

We have now to check that all four trajectories above verify the geometric constraints imposed by the inputs.

Property: The four primitives described above are trajectories γ lying at a distance less than ϵ from S_1 and S_2.

Proof: The proof comes from the choice of the intermediate configuration c lying on the bisector of segments S_1 and S_2, and from the convexity of the arcs of clothoids and anticlothoids used to construct γ in each case.

Consider the "tube" consisting of all the points whose distance to S_1 and S_2 is less than ϵ. It is bounded by:

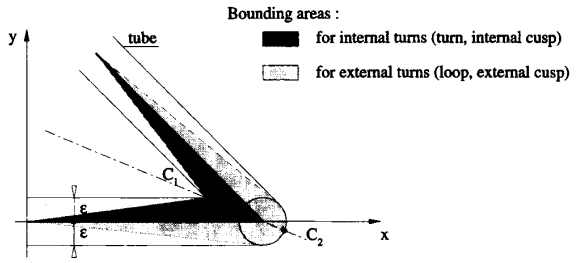

Fig. 10. The trajectory γ lies inside the tube of width ϵ.

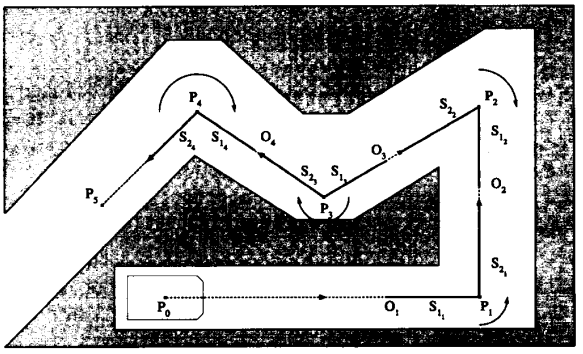

Fig. 11. A directed broken line.

- two segments intersecting at point C_1 with coordinates $(e - \epsilon \cot \frac{\alpha}{2}, \epsilon)$, and
- two segments and an arc of a circle intersecting the bisector at point C_2 with coordinates $(e + \epsilon \cos \frac{\alpha}{2}, -\epsilon \sin \frac{\alpha}{2})$.

In the cases of the internal cusp and the turn, the intermediate configuration lies at point C_1. From convexity arguments, the portion of γ from the origin to c lies under the line (OC_1) and over the x-axis, and therefore inside the tube (Fig. 10).

Similarly, in the cases of the loop and the external cusp, the portion of γ from the origin to c lies over the line (OC_2) and under the x-axis. This suffices to conclude for the case of the external cusp. For the loop, we can check that the curvature of γ at configuration c is less than ϵ. Thus, the first portion lies inside the convex part of the domain bounded by the arc of circle centered at P and of radius ϵ. Therefore, it lies inside the tube. By symmetry with respect to the bisector, the second portion of γ also lies inside the tube. □

Remark: Note that not only γ is close to the segments in the Cartesian space, but the corresponding path *in the configuration space* is also as close as we want to the initial path supported by the two segments and the rotation at P. Indeed the angular variation of the robot's orientation moving along γ is exactly the same as the initial angular variation along (S_1, P, S_2). This point is very important in constrained space when collision risks are due to the rotations.

V. Algorithm For Smoothing a Broken Line

In this section we show how to use the primitives above to smooth a reference path consisting of a collision-free directed broken line. The control laws are then deduced.

A. Smoothing a Broken Line

Let us consider a collision-free path consisting of a directed broken line (Fig. 11).

To make the smoothing of two consecutive turns independent, we compute for the segments $[P_{i-1}, P_i]$ and $[P_i, P_{i+1}]$ the point O_i

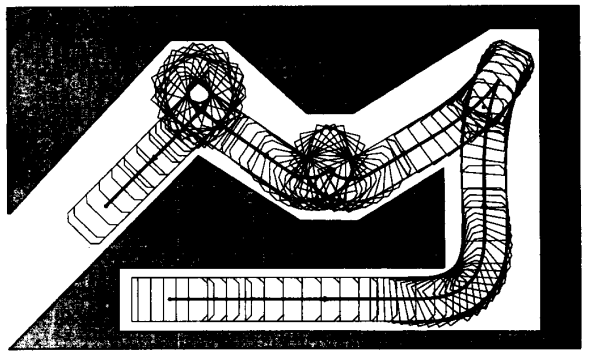

Fig. 12. Execution of the trajectory inferred from the broken line of Fig. 11.

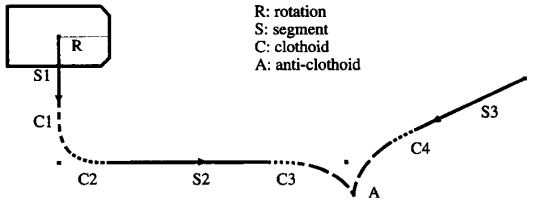

Fig. 13. A trajectory.

such that $\|O_iP_i\| = Min(\frac{\|P_{i-1}P_i\|}{2}, \frac{\|P_iP_{i+1}\|}{2})$. Then we use the smoothing procedure above, setting the first input segment of the smoothing primitives to $S_{1i} = [O_i, P_i]$.

B. Control Laws

All the above computations are based on the geometric properties of the clothoids and the anticlothoids. Recall that these curves are fully characterized by the parameters k_c and k_a. From the kinematic viewpoint, they can be expressed as functions of the velocities v_0 and ω_1, and the constant acceleration a:

$$\begin{cases} k_c = 2a/dv_0^2 \\ k_a = a/\omega_1^2 \end{cases}$$

Once a is set to the maximum acceleration, the speeds v_0 and ω_1 are obtained from the previous system. If v_0 (respectively, ω_1) exceeds its limit v_{0max} (respectively, ω_{1max}) it is set to v_{0max} (respectively, ω_{1max}) and a and ω_1 (respectively, v_0) are recomputed. The speed $v_{0_{i+1}}$ of a turn is also limited by the speed of the previous turn v_{0_i} and the capacity of acceleration between the turns (e.g. the length between the turns and the acceleration a).

C. Experiments

The smoothing method was implemented on the mobile robot Hilare 2. Fig. 12 shows an example trajectory that was actually executed and the swept space during motion.

The computation time takes less than 0.3 ms for a turn without cusp and less than 5 ms for a turn with a cusp on a 68040 cpu board with a 25 MHz clock.

Fig. 13 shows a trajectory portion with its different primitives. The trapezoidal speed profiles for this trajectory are shown on Fig. 13 (the maximum speeds were fixed to $v_1 = 0.5m/s$ and $\omega_0 = 0.95rd/s$).

The geometric characteristics and the admissible velocities and acceleration of the primitives along the trajectory (constants x_0, k_c and k_a and the length of each primitive) are determined before starting the motion. However, the computation of the geometric parameters is fast enough to envisage to do it on line. This could

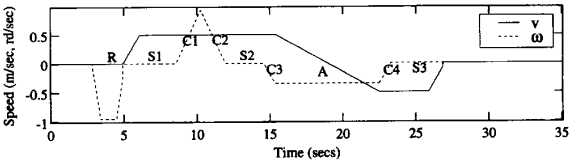

Fig. 14. Speed profile for the trajectory of Fig. 13 (the motion starts at 3 secs).

make it possible to link trajectories without stopping. The current reference point and velocities are updated in real time every 25 ms.

Remark: This method does not impose a constant acceleration. It is possible to change the speed profile dynamically while staying on the trajectory, by maintaining the instantaneous computed curvature radius. This allows for example to reduce speed or to stop the robot along the trajectory.

VI. Conclusion

We have introduced in this paper the use of the involutes of a circle to smooth paths described as broken lines that include a change in robot direction.

The combination of these curves - dubbed anticlothoids - and clothoids enable to produce a trajectory without discontinuities in the angular or linear velocities. The primitives presented in this paper allow a smooth complex motion and may have various applications.

We have addressed the case of a sequence Translation-Rotation-Translation because of its practical interest since most trajectory planners generate broken line paths. The same approach would have been also possible for the case Rotation-Translation-Rotation. The produced smooth trajectory would pass through the vertices of the reference trajectory, instead of the midpoints of its segments.

One difficulty for smoothing a broken line is to decide when to start a turn on the segment. The chosen heuristic has the advantage to make independent two consecutive turns, sometimes at the expense of increasing the trajectory execution time.

The "bang-bang" control has the advantages of local optimality and simplicity of the control law. Compliance with the kinematic constraints and with the speed limit guarantee the feasibility of the computed motion. As a consequence there is no noticeable deviation from the odometry measurements (computed for the feedback control) during execution.

We recall that even if the smoothing was produced by "bang-bang" commands, this does not guarantee the optimality of the trajectory.

Appendix
Equations of the Anticlothoid

In this Appendix, we present the computation of the configuration $c(t)$ of a mobile robot moving along an anticlothoid γ from a start configuration $c_0 = (x_0, y_0, \theta_0)$ with initial linear and angular velocities v_0 and ω_0.

The coordinates of $c(t)$ are

$$\begin{cases} x(t) &= \int_0^t v(u)\cos\theta(u)\,du &+ x_0 \\ y(t) &= \int_0^t v(u)\sin\theta(u)\,du &+ y_0 \\ \theta(t) &= \int_0^t \omega(u)\,du &+ \theta_0 \end{cases}.$$

From the definition of anticlothoids (see Section III-C), we have $\omega(t) = \omega_0$ and $v(t) = at + v_0$. Moreover the characteristic parameter of the anticlothoid is $k_a = \frac{a}{\omega_0^2}$. Thus:

$$\begin{cases} x(t) &= \int_0^t (au + v_0)\cos(\omega_0 u + \theta_0)\,du &+ x_0 \\ y(t) &= \int_0^t (au + v_0)\sin(\omega_0 u + \theta_0)\,du &+ y_0 \\ \theta(t) &= \omega_0 t &+ \theta_0 \end{cases}$$

By using an integration by parts, the coordinates $x(t)$ and $y(t)$ as functions of $\theta(t)$ are

$$\begin{aligned} x(t) &= k_a(\cos\theta - \cos\theta_0 + (\theta - \theta_0 + \tfrac{\omega_0 v_0}{a})\sin\theta \\ &\quad - \tfrac{\omega_0 v_0}{a}\sin\theta_0) + x_0 \\ y(t) &= k_a(\sin\theta - \sin\theta_0 - (\theta - \theta_0 + \tfrac{\omega_0 v_0}{a})\cos\theta \\ &\quad + \tfrac{\omega_0 v_0}{a}\cos\theta_0) + y_0 \\ \theta(t) &= \omega_0 t + \theta_0 \end{aligned}$$

When $v_0 < 0$, there is a point $\gamma(t)$ such that $v(t) = 0$. This is a cusp. The corresponding configuration $\hat{c}$ verifies

$$x_{\hat{c}} = k_a(\cos\theta_{\hat{c}} - \cos\theta_0 + (\theta_{\hat{c}} - \theta_0)\sin\theta_0) + x_0 \quad (11)$$

$$y_{\hat{c}} = k_a(\sin\theta_{\hat{c}} - \sin\theta_0 - (\theta_{\hat{c}} - \theta_0)\cos\theta_0) + y_0 \quad (12)$$

$$\theta_{\hat{c}} = -\frac{v_0\omega_0}{a} + \theta_0 \quad (13)$$

ACKNOWLEDGMENT

The authors are grateful to Matthieu Herrb for his help, especially in producing the graphic interface.

REFERENCES

[1] J. Iijima, Y. Kanayama, and S. Yuta, "A locomotion control system for mobile robots," in *7th Int. Joint Conf. Artificial Intell. (IJCAI),* 1981.
[2] H. Chochon and B. Leconte, "Etude d'un module de locomotion pour un robot mobile," in Rapport de fin d'étude ENSAE, Laboratoire d'Automatique et d'Analyse des Systèmes (C.N.R.S.), , 1983.
[3] Y. Kanayama and N. Miyake, "Trajectory generation for mobile robots," in *Robotics Research 3*, G. Giralt and O. Faugeras, Eds. Boston, MA: MIT Press, 1986.
[4] James and James, *Mathematics Dictionary.* Princeton, NJ: Van Nostrand, 1968.
[5] P. Jacobs, A. Rege, and J.-P. Laumond, "Non-holonomic motion planning for hilare-like mobile robot," in *Int. Symp. Intell. Robot. (ISIR),* 1991.
[6] P. Hartman, "The highway spiral for combining curves of different radii," *Trans. Amer. Soc. Civil Eng.*, 1957.
[7] D. Meek and D. Walton, "Clothoid spline transition spirals," *Math. Computation*, vol. 59, no. 199, July 1992.
[8] F. Noreils, A. Khoumsi, G. Baugil, and R. Chatila, "Reactive processes for mobile robot control," in *4th ICAR '89,* 1989.
[9] D. Shin and S. Singh, "Path generation for robot vehicules using composite clothoid segments," Technical Report CMU-RI-TR-90-31, Robotics Institute, Carnegie Mellon University, 1990.
[10] Y. Kanayama and B. Hartman, "Smooth local planning for autonomous vehicles," in *IEEE Int. Conf. on Robot. and Automat.,* 1989.
[11] H. Delingette, M. Herbert, and K. Ikeuchi, "Trajectory generation with curvature constraint based on energy minimization," in *IEEE Int. Workshop on Intell. Robots and Syst. (IROS '91),*, 1991.
[12] A. Segovia, M. Rombaut, A. Preciado, and D. Meizel, "Comparative study of the different methods of path generation for a mobile robot in a free environment," in *ICAR '91,* 1991.
[13] R. Chatila, "Mobile robot navigation: space modeling and decisional processes," in *Robotics Research: The Third Int. Symp.*, , 1985.
[14] L. Pontryagin, V. Boltyansky, R. Gamkrelidze, and E. Mischenko, *The Mathematical Theory of Optimal Processes.* New York: Wiley, 1962.
[15] D. Reister and F. Pin, "Time optimal trajectories for mobile robots with two independently driven wheels," *Int. J. Robot. Res.*, vol. 13, 1994.
[16] P. Souères and J. P. Laumond, "Shortest path synthesis for a car-like robot," in *European Cont. Conf.,* 1993.
[17] J. P. Laumond, T. Simeon, R. Chatila, and G. Giralt, "Trajectory planning and motion control for mobile robots," in *Geometry and Robotics,*, J. D. Boissonnat and J. P. Laumond, Eds. (Lecture Notes in Computer Science, Vol. 391). New York: Springer Verlag, 1989, pp. 133–149.
[18] J. P. Laumond, P. E. Jacobs, M. Taïx, and R. M. Murray, "A motion planner for nonholonomic mobile robots," *IEEE Trans. Robot. and Automat.,* vol. 10, no. 5, pp. 577–593, 1994.

Real-Time Collision Avoidance for Redundant Manipulators

K. Glass, *Member, IEEE*, R. Colbaugh, *Member, IEEE*, D. Lim, and H. Seraji, *Senior Member, IEEE*,

***Abstract*—This paper presents a simple and robust approach to achieving collision avoidance for kinematically redundant manipulators at the control-loop level. The proposed scheme represents the obstacle avoidance requirement as inequality constraints in the manipulator workspace, and ensures that these inequalities are satisfied while the end-effector tracks the desired trajectory. The control scheme is the damped-least-squares formulation of the configuration control approach implemented as a kinematic controller. Computer simulation and experimental results are given for a Robotics Research 7 DOF redundant arm and demonstrate the collision avoidance capability for reaching inside a truss structure. These results confirm that the proposed approach provides a simple and effective method for real-time collision avoidance.**

I. INTRODUCTION

In Oct. 1990, the National Aeronautics and Space Administration (NASA) initiated a research and development project on Remote Surface Inspection (RSI) at the Jet Propulsion Laboratory (JPL). The goal of this project is to develop and demonstrate the necessary technologies for the inspection of space structures, such as the Space Station Freedom (SSF), using remote robots for sensor placement under supervisory control. The purpose of the inspection is to monitor the health of the structure and assess possible damage by employing a number of sensing devices deemed appropriate for the task. Fig. 1 shows the Surface Inspection Laboratory which emulates the task environment where the inspection will be performed. This figure shows a one-third scale mock-up of part of the truss structure of SSF, as well as a seven degree-of-freedom (DOF) Robotics Research Corporation (RRC) manipulator that carries the inspection sensors at its end-effector. Complete inspection of the truss structure and the orbital replacement units mounted on it requires the capability to reach safely into the truss openings and to maneuver in constricted workspaces inside the truss. Therefore, the ability to perform automated collision-free motions in a congested environment is a fundamental requirement for the project.

The robotic arm used in the project is kinematically redundant since it possesses more DOF than are required to achieve the desired position and orientation of the end-effector. One of the advantages of robot redundancy is the potential to use the "extra" DOF to maneuver in a congested workspace and avoid collisions with obstacles. Much of the work reported to date concerning collision avoidance for manipulators has dealt with high-level *path planning*, in which the end-effector path is planned *off-line* so as to avoid collision with workspace obstacles (see, for example, the recent text [1] and the references therein). Alternatively, the obstacle avoidance problem can be solved *on-line* by the robot controller at the low level. Previous approaches to on-line obstacle avoidance for redundant manipulators have focused on the inverse kinematics portion of the robot control problem (e.g., [2]-[7]), although Khatib [8] and Colbaugh *et al.*

Manuscript received August 20, 1993; revised July 5, 1994.

K. Glass and R. Colbaugh are with the Department of Mechanical Engineering, New Mexico State University, Las Cruces, NM 88003 USA.

D. Lim and H. Seraji are with the Jet Propulsion Laboratory, California Institute of Technology, Pasadena, CA 91109 USA.

IEEE Log Number 9410112.